Cytochrome *c* conformations resolved by the photon counting histogram: Watching the alkaline transition with single-molecule sensitivity

Thomas D. Perroud, Michael P. Bokoch, and Richard N. Zare*

Department of Chemistry, Stanford University, Stanford, CA 94305-5080

Contributed by Richard N. Zare, October 13, 2005

We apply the photon counting histogram (PCH) model, a fluorescence technique with single-molecule sensitivity, to study pH-induced conformational changes of cytochrome *c*. PCH is able to distinguish different protein conformations based on the brightness of a fluorophore sensitive to its local environment. We label cytochrome *c* through its single free cysteine with tetramethylrhodamine-5-maleimide (TMR), a fluorophore with specific brightnesses that we associate with specific protein conformations. Ensemble measurements demonstrate two different fluorescence responses with increasing pH: (*i*) a decrease in fluorescence intensity caused by the alkaline transition of cytochrome *c* (pH 7.0–9.5), and (*ii*) an increase in intensity when the protein unfolds (pH 9.5–10.8). The magnitudes of these two responses depend strongly on the molar ratio of TMR used to label cytochrome *c*. Using PCH we determine that this effect arises from the proportion of a nonfunctional conformation in the sample, which can be differentiated from the functional conformation. We further determine the causes of each ensemble fluorescence response: (*i*) during the alkaline transition, the fluorophore enters a dark state and discrete conformations are observed, and (*ii*) as cytochrome *c* unfolds, the fluorophore incrementally brightens, but discrete conformations are no longer resolved. Moreover, we also show that functional TMR-cytochrome *c* undergoes a response of identical magnitude regardless of the proportion of nonfunctional protein in the sample. As expected for a technique with single-molecule sensitivity, we demonstrate that PCH can directly observe the most relevant conformation, unlike ensemble fluorometry.

single-molecule fluorescence spectroscopy | protein conformations | protein labeling | confocal microscopy | metalloprotein

In cellular signaling networks, rare conformations of proteins are believed to be crucial for determining outcomes of the entire system (1, 2). Traditional biophysical methods rely on ensemble averages, that is, measurements from a large number of molecules simultaneously. As a consequence, rare, but important, populations can be obscured and go undetected. Recent advances in single-molecule methodology have allowed researchers to break the ensemble average and more thoroughly characterize the heterogeneity of biological samples (3). This report describes the application of the photon counting histogram (PCH) model (4–7), a fluorescence spectroscopy technique with single-molecule sensitivity, to study the conformational heterogeneity of cytochrome *c* as a function of pH.

Fluorescence spectroscopy has long been an important methodology for studying the conformational states of proteins, which is commonly done either by measuring the intrinsic fluorescence of the protein (for example, tryptophan residues) or covalently attaching an external fluorophore to specific residues (8). The latter approach assumes that the fluorophore does not significantly perturb the protein under investigation and that the photophysical properties of a fluorescent probe are sensitive to the local environment. Different environments generated by different protein conformations give rise to changes in the fluorescence signal. Thus, the fluorescence intensity can be correlated with protein conformation. The standard approach for determining conformational heterogeneity is to record the fluorescence from many biomolecules as a function of time. However, such measurements can only report an ensemble average. In contrast, PCH has the advantage of observing molecules one at a time, thus exploiting the sensitivity of single-molecule fluorescence spectroscopy to detect the presence of rare conformations.

PCH operates by recording the fluorescent bursts as molecules at nanomolar concentration diffuse through the tightly focused laser beam (volume <1 fl) of a confocal microscope. Whereas fluorescence correlation spectroscopy (9, 10) analyzes the fluctuations in fluorescence with time, PCH analyzes the fluctuations in fluorescence amplitude. PCH distinguishes different fluorescent species based on the brightness ε of the fluorophore, a parameter that includes its absorbance cross section and its fluorescence quantum yield (4, 5). If different brightnesses correspond to specific protein conformations, PCH can resolve the heterogeneity of conformational states with single-molecule sensitivity. Using the PCH model for one-photon excitation for confocal microscopy, we successfully resolved a mixture of fluorophores characterized by different brightnesses (5, 6). We also studied the effect of time-dependent processes (such as diffusion and triplet formation) on the PCH parameters and determined optimal experimental conditions to minimize the influence of these processes (7). This article shows the application of this method for detecting protein conformational states. As a model system, we chose iso-1-cytochrome *c* from the yeast *Saccharomyces cerevisiae*. Cytochrome *c* is a soluble protein with a heme prosthetic group that is involved in mitochondrial electron transport. This model protein has served as a template for the introduction of new spectroscopic methods over the past five decades (11), and thus represents an ideal target for demonstrating the power of PCH to characterize biological macromolecules.

To study the conformational changes of cytochrome *c* with pH, the protein is labeled with a conformationally sensitive fluorescent probe, tetramethylrhodamine-5-maleimide (TMR), through its single free cysteine residue. We first show that PCH can be used to thoroughly characterize the labeling process. We then show that PCH is able to distinguish functional from nonfunctional conformations of TMR-cytochrome *c*, unlike ensemble fluorometry. Finally, we use PCH to observe and characterize two known pH-induced conformational changes regardless of background interference.

Experimental Procedures

Labeling and Purification of Cytochrome *c*. The buffer used for all experiments (except MS) consisted of 25 mM sodium phosphate (pH 7.0), 25 mM 2-(cyclohexylamino)ethanesulfonic acid (Sigma),

Conflict of interest statement: No conflicts declared.

Abbreviations: PCH, photon counting histogram; TMR, tetramethylrhodamine-5-maleimide; cpbm, counts per bin time per molecule.

*To whom correspondence should be addressed. E-mail: zare@stanford.edu.

www.pnas.org/cgi/doi/10.1073/pnas.0508975102

and 200 mM sodium chloride. This two-component buffer yields a nearly linear titration curve from pH 7.0 to 10.8, and 200 mM sodium chloride ensures that the change in ionic strength (<20%) has minimal effect on fluorescence (<1%) during a titration in this range. Iso-1-cytochrome *c* from the yeast *S. cerevisiae* (Sigma) was dissolved in buffer at a concentration of 3.0 mg/ml and labeled with TMR (Invitrogen) at various molar ratios of TMR/cytochrome *c* (1:50, 1:10, 1:5, and 2:1 labeling molar ratios). Each labeling mixture was protected from light and incubated at room temperature for 3 h with gentle mixing. The TMR-cytochrome *c* conjugate was thoroughly purified from unreacted fluorophore by size exclusion chromatography (Sephadex G-25 Fine Grade, 1 × 25-cm bed, Sigma). TMR-cytochrome *c* eluted as a single band (monitored by the Soret absorbance at 410 nm) that was separated from unreacted TMR by at least 15 cm on the column.

TMR-cytochrome *c* was characterized by using UV-visible spectrophotometry, CD, ensemble fluorometry, and MS by using standard methods (*Supporting Text*, which is published as supporting information on the PNAS web site). The protocols for trypsin digestion and pH titrations are also described therein.

Confocal Microscopy. The confocal microscope was similar to that described (7), with the following modifications. All experiments were performed with a water immersion objective (Plan Apo ×60 numerical aperture = 1.20, Nikon) and a 50-μm pinhole. One emission filter (595AF60, Omega Optical, Brattleboro, VT) was used between the pinhole and the avalanche photodiode detector (SPCM, EG & G, Salem, MA). Autocorrelation functions were obtained from a digital correlator (Flex99R-480, Correlator.com, Bridgewater, NJ). The data acquisition time was 800 s for all PCH experiments and 20 s for each autocorrelation function. The power of the diode-pumped frequency-doubled Nd:YAG laser (532 nm, Coherent, Santa Clara, CA) was ≈100 μW at the sample. Protein samples for confocal experiments were held in 8-well Labtek II coverglass chambers (Nalge/Nunc). The glass surface was cleaned by sonication in 1 M potassium hydroxide for 15 min, followed by a rinse and 5-min sonication in Milli-Q water and a final rinse. Sample wells were incubated for 2 h at room temperature with a solution of unlabeled cytochrome *c* in buffer (1.0 mg/ml) to coat the surface and prevent adsorption of TMR-cytochrome *c*. The unlabeled protein solution was pipetted from each well just before the addition of TMR-cytochrome *c* (5–50 nM). Imaging the glass surface with an intensified charge-coupled device camera showed that this treatment was effective in blocking protein adsorption (data not shown).

PCH Model for One-Photon Excitation and Data Analysis. The construction of the PCHs for a given bin time and the determination of the resulting PCH parameters were similar to methods as described (6). Using fluorescence correlation spectroscopy, we determined a triplet relaxation time of 8 μs, a triplet fraction of 15%, and a diffusion time of 96 μs for TMR-cytochrome *c*. We chose a bin time of 20 μs so that triplet formation and diffusion did not influence the PCH parameters by >10% (7). All histograms were fitted with one, two, and three species by using a second-order correction for the PCH model (6). The best model was chosen based on the goodness of the fit and the proper value for the semiempirical parameter $F = 0.67 \pm 0.07$, which characterizes the deviation of the observation volume from a 3D Gaussian volume (5). Sometimes the addition of a third species (very rare and very bright) improved the goodness of the fit. This species was interpreted as either an aggregate or a deviation from the nonideality of the PCH model. Nevertheless, the third species was not considered during data interpretation, because adding it did not numerically change the values of the PCH parameters for the first two species. For all PCH parameters, the number of significant figures is set according to the estimated SD of each fitting parameter (for a more detailed description of the fitting procedure, see *Supporting Text*, Fig. 7, and Table 4, which are published as supporting information on the PNAS web site).

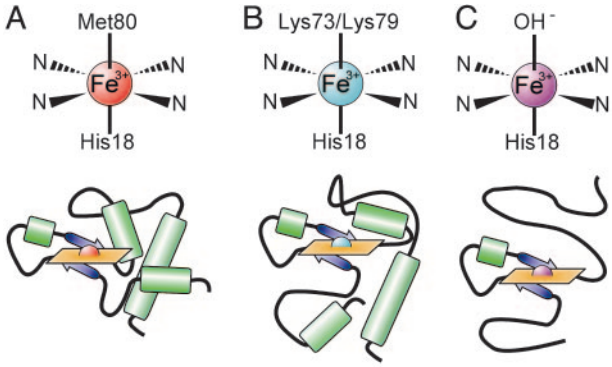

Fig. 1. Heme ligation schemes (*Upper*) and structural models (*Lower*) for ferricytochrome *c* state III (*A*), state IV, the alkaline state (*B*), and state V, unfolded (*C*). Two possible alkaline conformers exist because either Lys-73 or Lys-79 can act as the sixth axial heme ligand.

Results and Discussion

The conformational changes of cytochrome *c* with pH have been well studied (12). In 1941, Theorell and Åkesson (13) demonstrated five spectrally resolvable states for the oxidized form of cytochrome *c* (ferricytochrome *c*) by using absorption spectrophotometry. The conformation present at neutral pH is defined by ligation of the heme iron by Met-80 in the sixth axial position (state III, Fig. 1*A*). Upon increasing pH, state III transforms to state IV, where one of two lysine residues, Lys-73 or Lys-79, replaces Met-80 as a heme ligand (Fig. 1*B*) (14, 15). This conformational change, called the "alkaline transition," has an apparent pK_a between 8.4 and 8.9 for yeast iso-1-cytochrome *c* (16). A further increase in pH causes drastic unfolding of the protein (Fig. 1*C*) (17), and the transition to this unfolded state (state V) occurs with a pK_a of 10.5–11.7 (16, 18). It remains controversial whether or not these alkaline conformers are biologically relevant. Using direct electrochemistry, Barker and Mauk (19) have shown a large decrease in reduction potential for cytochrome *c* in state IV. Other experiments hint at structural similarities between these alkaline conformers and cytochrome *c* bound to cytochrome *c* oxidase; for a discussion, see Rosell *et al.* (20) and Döpner *et al.* (18). Regardless, these well characterized conformational changes provide a robust model system for application of PCH.

Tetramethylrhodamine Fluorescence Reports on the pH-Dependent Conformational Changes of Cytochrome *c* When Conjugated to Cys-102. Yeast iso-1-cytochrome *c* has a single free cysteine residue (Cys-102) that should ensure site-specific labeling (one fluorophore per protein) with a maleimide functionalized fluorophore (TMR). Multiple labeling possibilities, characterized by multiple brightnesses ε_i, would introduce undesired heterogeneity in the number of fluorescent species present in the sample. The presence of a bright doubly labeled species could obscure subtle differences in brightness originating from conformational heterogeneity, and thus confound interpretation.

We have chosen TMR, a small organic fluorophore, because it disturbs the native structure of the protein to a lesser degree than large polypeptides such as green fluorescent protein. Cys-102 is buried from solvent in a hydrophobic pocket, and a partial unfolding of cytochrome *c* must occur before labeling (21, 22). Furthermore, modification of Cys-102 by alkylation or protein dimerization is known to perturb the spectral, chemical, and physical properties of the molecule (22). It is therefore essential to determine the functional and structural integrity of the protein after TMR modification. For this purpose, cytochrome *c* was labeled at pH 7.0 with

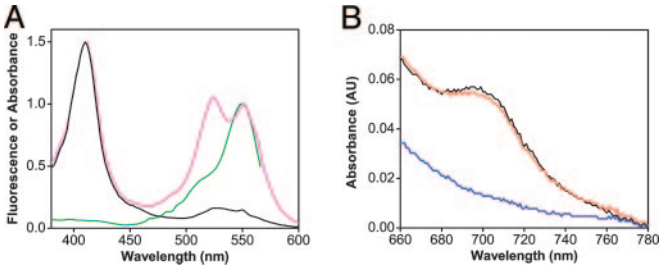

Fig. 2. Characterization of TMR-cytochrome *c* by fluorescence and UV-visible spectroscopy. (*A*) Absorbance and fluorescence spectra of unlabeled and labeled cytochrome *c*. Normalized absorbance spectra of unlabeled cytochrome *c* (black) and cytochrome *c* labeled with a 2:1 molar ratio of TMR (magenta). The fluorescence excitation spectrum of TMR-cytochrome *c* (green) shows that the absorbance peak at 550 nm is fluorescent. (*B*) The 695-nm absorbance band of cytochrome *c* characteristic of Met-80 ligation is present at pH 7.0 (black) and is abolished at pH 9.5 (blue). Subsequent addition of HCl restores the 695-nm absorbance band (red).

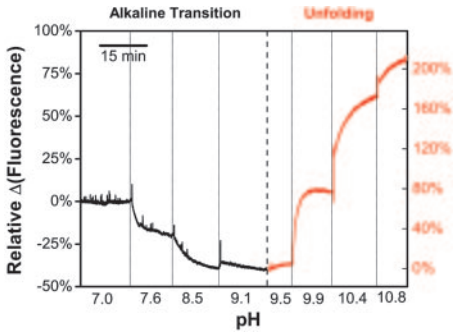

Fig. 3. The fluorescence of TMR-cytochrome *c* (labeled at a 1:5 molar ratio) indicates pH-induced conformational changes. The ensemble fluorescence consists of two responses: a decrease in fluorescence from pH 7.0 to 9.1 (the alkaline transition, black) followed by an increase in fluorescence from pH 9.5 to 10.8 (cytochrome *c* unfolds, red).

a 2:1 molar excess of TMR to ensure high labeling efficiency. After the labeling reaction and purification by size-exclusion chromatography, the absorbance spectrum of TMR-cytochrome *c* in state III (Fig. 2*A*) shows three peaks: (*i*) the heme Soret band at 412 nm; (*ii*) a nonfluorescent TMR peak at 525 nm; and (*iii*) a fluorescent TMR peak at 550 nm. The difference in shape between the absorbance and fluorescence excitation spectra suggests that cytochrome *c* is labeled with multiple fluorophores (23). This prediction is confirmed by a calculated labeling efficiency of ≈1.2 fluorophores per protein for the sample shown in Fig. 2*A* (for a discussion on the TMR-cytochrome *c* absorbance spectrum: see *Supporting Text* and Figs. 8 *A–C* and 9 *A–C*, which are published as supporting information on the PNAS web site). This result is unexpected. It implies that the protein is being labeled at another site in addition to Cys-102. Nevertheless, we conclude that nearly 100% of cytochrome *c* monomers (see below) are labeled with at least one fluorophore, making this sample adequate for characterizing protein structure and function.

CD was used to characterize the secondary structure of cytochrome *c* and ensure that the protein backbone is not drastically disturbed by the presence of TMR. The far-UV CD spectrum of unlabeled cytochrome *c* shows the double peak expected for a protein with predominately α-helical structure (24). The spectrum for TMR-cytochrome *c* is less intense but shows a similar α-helical signature (Fig. 10, which is published as supporting information on the PNAS web site). A decrease in intensity of the CD spectrum is consistent with modification of Cys-102 by disulfide dimerization (25), a condition under which the protein is still functional (22, 26). From these results we conclude that the polypeptide backbone of cytochrome *c* is not majorly disrupted in the presence of TMR.

The absorbance spectrum of cytochrome *c* displays a weak band at 695 nm that is highly specific for the correctly folded and functional form of the protein. This band is diagnostic for intact Met-80 ligation of the heme iron and is used to define state III in a spectroscopic manner (12, 13). Only state III of ferricytochrome *c* is functional and reducible under physiological conditions (17). Fig. 2*B* shows the presence of a 695-nm absorbance band for TMR-cytochrome *c* at pH 7.0, which confirms that the labeled protein is correctly folded. The alkaline transition of cytochrome *c* is traditionally monitored by the disappearance of this absorbance band at increasing pH, as Met-80 becomes displaced by lysine as the heme axial ligand (27). As shown in Fig. 2*B*, the 695-nm absorbance is removed by the addition of sodium hydroxide and reversed upon addition of hydrochloric acid. The pK_a of this transition was measured as 8.64 ± 0.03 for unlabeled cytochrome *c* and 8.09 ± 0.08 for TMR-cytochrome *c*, in agreement with Moench and Satterlee (22) who observed a decrease in pK_a upon covalent modification of Cys-102. These results demonstrate that TMR-cytochrome *c* retains its functionality with regard to the alkaline conformational change.

The fluorescence intensity of TMR-cytochrome *c* was measured by ensemble fluorometry as a function of pH, to verify that the fluorophore reports on pH-dependent conformations. As shown in Fig. 3, the ensemble fluorescence of TMR-cytochrome *c* shows two different responses during titration with sodium hydroxide: a decrease in intensity from pH 7.0 to pH 9.5, followed by a larger increase in intensity from pH 9.5 to pH 10.8. Each fluorescence response is reversible upon addition of hydrochloric acid, consistent with the reversibility of the 695-nm absorbance band (Fig. 2*B*). The decrease in intensity is interpreted as the alkaline transition, and the increase in intensity observed at higher pH is interpreted as the unfolding of cytochrome *c*. Additionally, the intensity changes are not accompanied by any shift in the fluorescence emission maximum (Fig. 9*C*), which suggests different degrees of quenching at different pH values. More importantly, TMR bound to free cysteine (TMR-cysteine) shows no response in the same pH range, which demonstrates that TMR is sensitive to pH only when bound to cytochrome *c* (Fig. 11, which is published as supporting information on the PNAS web site). We therefore conclude that TMR-cytochrome *c* is properly folded and functional, and its fluorescence reports on pH-induced conformational changes.

Heterogeneity from Sample Preparation. The magnitude of the fluorescence response for the alkaline transition depends strongly on the molar ratio of TMR used to label cytochrome *c*. To elucidate the reason behind this behavior, we prepared four samples with different labeling molar ratios between TMR and cytochrome *c* (2:1, 1:5, 1:10, and 1:50). The 1:5 labeling molar ratio gives the largest decrease (−49%), followed by 1:10 (−22%), 1:50 (−13%), and finally 2:1 (−5%) (Table 1). Each sample was analyzed on an ensemble level by electrospray ionization-MS and on the single-molecule level with PCH.

Characterization of the labeling step by MS. For all four samples mentioned above, three possible molecular masses were ob-

Table 1. Anticorrelation between the ensemble fluorescence response for the alkaline transition (Δ*I*) and the contribution of species 2 to the total fluorescence intensity (S_2)

	Molar ratio of TMR/cytochrome *c*			
Parameter	1:5	1:10	1:50	2:1
Δ*I*	−49%	−22%	−13%	−5%
S_2	13% ± 5%	17% ± 3%	29% ± 4%	45% ± 10%

Table 2. MS results on four samples labeled with different molar ratios of TMR/cytochrome *c*

	Molar ratio of TMR/cytochrome *c*			
Peak present in mass spectrum	1:50	1:10	1:5	2:1
Unlabeled cytochrome *c*	+	+	+	+
Singly labeled cytochrome *c*		+	+	+
Doubly labeled cytochrome *c*				+

served on the mass spectra and are interpreted as either unlabeled, singly labeled, or doubly labeled cytochrome *c* (*Supporting Text*). As shown in Table 2, MS is not sensitive enough to detect TMR-cytochrome *c* in a sample labeled at a 1:50 labeling molar ratio. For the 1:10, 1:5, and 2:1 labeling molar ratios, MS detects unlabeled and singly labeled cytochrome *c*. Doubly labeled cytochrome *c* appears only in the sample labeled at a 2:1 molar ratio.

Although surprising for a protein with only one free cysteine, the presence of doubly labeled cytochrome *c* is consistent with the previously determined labeling efficiency (≈1.2 fluorophores per protein, Fig. 2*A*). The other two cysteines in cytochrome *c*, Cys-14 and Cys-17, are covalently bound to the heme group and inaccessible to labeling (21). We believe that the second molecule of TMR nonspecifically labels amines on the protein when Cys-102 is no longer available (28). This residue also becomes inaccessible to labeling when cytochrome *c* dimerizes through Cys-102 (29), thus explaining the presence of unlabeled cytochrome *c* in the mass spectrum of the 2:1 labeled sample. In electrospray ionization-MS experiments the molecular masses of charged monomers and doubly charged dimers are indistinguishable, because the resulting mass-to-charge ratios are too similar to be experimentally resolved. We conclude that using an excess of protein in the labeling step ensures selectivity for Cys-102 and essentially eliminates double labeling.

Characterization of the labeling step using PCH. Using PCH we determine the number of fluorescent species, characterized by different brightnesses ε_i [units: counts per bin time per molecule (cpbm)], and their respective abundance, characterized by $\bar{N}_i$, for the same four samples mentioned above (pH 7.0). We combine these results with those obtained by MS to identify each species.

When an excess of protein is used during the labeling reaction (1:50 labeling molar ratio), PCH is sensitive enough to detect TMR-cytochrome *c* as expected for a technique based on fluorescence, whereas MS cannot. Using PCH we observe two fluorescent species, for which we arbitrarily assign numbers in order of increasing brightness (Table 3). Species 1, defined by ε_1, is the dimmest ($\varepsilon_1 = 0.43$ cpbm) and most abundant species. Species 2, defined by ε_2, is brighter ($\varepsilon_2 = 2.38$ cpbm) and less abundant. To verify that these two species are real and not artifacts from improper fitting, a few tests were performed. First, the average number of molecules $\bar{N}_i$ correlates linearly with the concentration for both species, while the brightness of each species ε_i remains constant. Second, ε_i correlates with laser power while $\bar{N}_i$ remains constant (Fig. 12 *A–D*, which is published as supporting information on the PNAS web site). Third, PCH only detects one species after protease digestion of TMR-cytochrome *c* with trypsin. With 19 potential sites for trypsin cleavage (30), this digest should completely destroy the tertiary structure of cytochrome *c* and reduce the number of fluorescent species to one, consistent with our observation. Additionally, the brightness of this single species is similar to TMR-cysteine, consistent with the notion that the fluorophore is no longer quenched. Because cytochrome *c* is in excess compared with TMR (1:50 labeling molar ratio), the probability of TMR-maleimide reacting nonspecifically with amines (usually lysines) is negligible. Thus, ε_1 and ε_2 are believed to represent two different conformational states of singly labeled cytochrome *c*. Species 1 is a conformation where the fluorophore is significantly quenched ($\varepsilon_1 \approx 0.4$ cpbm). Species 2 is a conformation where the fluorophore is not quenched and has a brightness similar to TMR-cysteine ($\varepsilon_2 \approx 2.7$ cpbm).

As the concentration of TMR used in the labeling reaction increases, more proteins are labeled and both species become more abundant with respect to the total concentration of cytochrome *c* (Table 3). However, $\bar{N}_1$ increases faster than $\bar{N}_2$ as illustrated by the ratio $\bar{N}_1/\bar{N}_2$. This behavior suggests different reactivities of the fluorophore toward the two different conformations. Assuming that the reaction between TMR and cytochrome *c* is complete after 3 h, species 2 must have a higher reactivity than species 1 for TMR to account for the increase in $\bar{N}_1/\bar{N}_2$ with increasing labeling molar ratio. Thus the possibility that species 2 represents labeling of a lysine residue can be ruled out. Additionally, $\bar{N}_1/\bar{N}_2$ increases over days (Fig. 13, which is published as supporting information on the PNAS web site) reinforcing the interpretation that species 1 and 2 are not simply cytochrome *c* molecules labeled at different sites. We conclude that species 1 and species 2 must represent two distinct conformations of cytochrome *c* when a substoichiometric amount of TMR is used during the labeling reaction.

When an excess of fluorophore is used during the labeling reaction (2:1 labeling molar ratio), we observe a radical change in the abundance of these two species. $\bar{N}_2$ suddenly becomes a significant proportion of the molecules ($\bar{N}_1/\bar{N}_2$ decreases by an order of magnitude to 5), in opposition to the trend observed for the previous three samples. We have shown by electrospray ionization-MS and UV-visible spectrophotometry that doubly labeled cytochrome *c* is present in the sample labeled at a 2:1 molar ratio. Therefore, the drastic increase in $\bar{N}_2$ is attributed to the appearance of doubly labeled cytochrome *c*. However, we also know that singly labeled molecules likely make up a small portion of $\bar{N}_2$ in this sample. At a 1:50 molar labeling ratio, we are certain that the observed molecules with brightness 2.38 cpbm have only a single label; these should be present in the 2:1 sample as well. Therefore species 2 in the 2:1 molar labeling ratio sample is a sum of both singly (unquenched) and doubly labeled protein. The fact that PCH cannot resolve these two labeling possibilities is explained by the

Table 3. PCH parameters at pH 7.0 from four samples labeled with different molar ratios of TMR/cytochrome *c*

	Molar ratio of TMR/cytochrome *c*			
Parameter	1:50	1:10	1:5	2:1
$\bar{N}_1$*	0.075 ± 0.004	0.58 ± 0.02	1.49 ± 0.07	3.9 ± 0.3
ε_1, cpbm	0.43 ± 0.05	0.40 ± 0.02	0.44 ± 0.04	0.72 ± 0.06
$\bar{N}_2$*	0.0055 ± 0.0004	0.020 ± 0.003	0.04 ± 0.01	0.8 ± 0.1
ε_2, cpbm	2.38 ± 0.09	2.4 ± 0.1	2.7 ± 0.3	2.8 ± 0.2
$\bar{N}_1/\bar{N}_2$	14 ± 1	29 ± 5	40 ± 10	5 ± 1
S_2	29% ± 4%	17% ± 3%	13% ± 5%	45% ± 10%

*$\bar{N}_1$ and $\bar{N}_2$ are normalized to the total concentration of cytochrome *c* for comparison between samples.

small difference in brightness between singly and doubly labeled TMR-cytochrome *c*. Before cytochrome *c* becomes doubly labeled, species 1 is the most abundant species in the sample ($\bar{N}_1/\bar{N}_2 > 40$). Therefore species 1 ($\varepsilon_1 \approx 0.4$ cpbm), which represents the quenched fluorophore, is the most likely to become labeled nonspecifically by a second fluorophore. This fluorophore is believed to be unquenched ($\varepsilon_i \approx 2.7$ cpbm), which makes the total brightness of this species ≈3.1 cpbm. Under the current experimental conditions, PCH cannot resolve two species when the brightnesses differ by only 15% (6, 31). Following the same logic, a third species should appear when the unquenched fluorescent species is labeled by another fluorophore. Because the unquenched fluorescent species is rare, the probability of this species getting a second label is unlikely.

PCH requires only a single fluorophore, making it a much simpler approach compared with techniques requiring two different fluorophores bound to a protein at two specific sites, such as single-pair fluorescence resonance energy transfer (32). PCH has allowed us to characterize the cytochrome *c* labeling process, which is found to be more complicated than might have been suspected. Although other approaches have been developed to circumvent challenges in site-specific labeling (33, 34), such techniques are not yet well established. PCH presents an appealing alternative to methods requiring multiple fluorophores.

Identifying Species 1 as the Functional Conformation of Cytochrome *c*. As described previously, the labeling molar ratio influences significantly the magnitude of the ensemble fluorescence response (Table 1). We have demonstrated that the 2:1 labeling molar ratio sample has both singly and doubly labeled cytochrome *c*. The presence of a second nonconformationally sensitive fluorophore adds more background and therefore decreases the ensemble fluorescence response. However, knowing that the 1:5, 1:10, and 1:50 labeling molar ratio samples have only singly labeled cytochrome *c*, the relative fluorescence response should remain constant. The observed results suggest that the 1:5 sample has the highest proportion of functional TMR-cytochrome *c*, whereas the 1:50 sample has the lowest. To understand this behavior, we break the averaging effect of ensemble measurements on the fluorometer and analyze the pH-induced conformational changes of TMR-cytochrome *c* with single-molecule sensitivity.

Fig. 4 shows the different results obtained by PCH for both the alkaline transition and the unfolding of cytochrome *c* for the 1:5 sample. We observe that species 1 and 2 are affected by pH in completely different ways. The average number of molecules $\bar{N}_1$ decreases by ≈56% in the pH range from 7.0 to 9.5 (Fig. 4*A*), while the brightness of species 1, ε_1, remains constant (Fig. 4*B*). After pH 9.5, both ε_1 and $\bar{N}_1$ start to increase significantly (110% and 150%, Fig. 4 *A* and *C*, respectively). On the other hand, species 2 is unaffected by the titration with sodium hydroxide. Indeed neither its brightness ε_2 (Fig. 4*B*) nor its abundance $\bar{N}_2$ (Fig. 4*A*) change with increasing pH, even during the unfolding of cytochrome *c*. We therefore identify species 1 as the functional conformation and species 2 as the nonfunctional conformation. Considering the nonfunctional nature of species 2 between pH 7.0 and 10.8, we speculate that species 2 is either unfolded cytochrome *c* (12) or the reduced form of the protein (ferrocytochrome *c*) (27) (for discussion, see *Supporting Text*).

Because species 2 represents a nonfunctional conformation, it contributes to the background and thus decreases the ensemble fluorescence response for both transitions. The contribution of species 2 to the total fluorescence intensity can be determined by $S_2 = \bar{N}_2\varepsilon_2/(\bar{N}_1\varepsilon_1 + \bar{N}_2\varepsilon_2)$. For the alkaline transition, S_2 is smallest at a 1:5 labeling molar ratio (13%), followed by 1:10 (17%), 1:50 (29%), and finally 2:1 (45%), as shown in Table 1. The increasing contribution of species 2 observed with PCH correlates well with the decreasing fluorescence response observed at the ensemble level. Using PCH we are able to distinguish the species contributing to the signal from those contributing to the background. It is therefore possible to observe the functional species directly without interference from background arising from nonfunctional conformations.

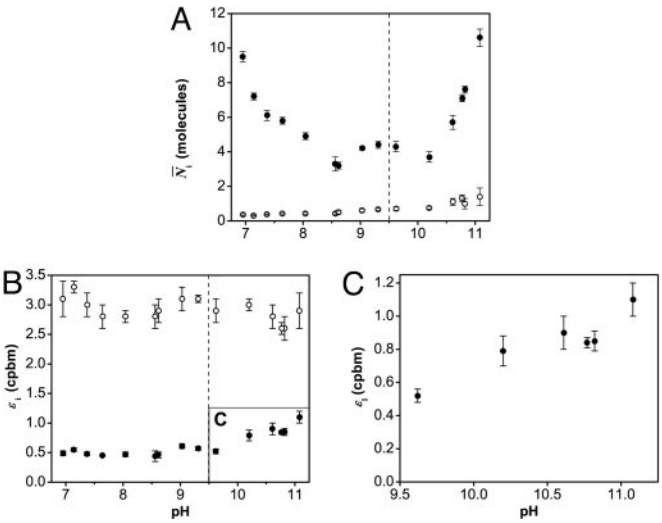

Fig. 4. PCH parameters of TMR-cytochrome *c* as a function of pH. These results explain the intensity changes seen by ensemble fluorometry (see Fig. 3) in terms of the parameters ε_i and $\bar{N}_i$ from a two-species fit (●, species 1; ○, species 2). The decrease in intensity during the alkaline transition (pH 7.0–9.5) is caused by a 56% decrease in $\bar{N}_1$ (*A*). The increase in intensity during unfolding (pH 9.5–10.8) is caused by a 150% increase in $\bar{N}_1$ (*A*) and a 110% increase in ε_1 (*B* and *C*). Neither the brightness nor the abundance of species 2 changes during the pH titration.

Analysis of pH-Induced Conformational Changes with PCH. ***Alkaline transition (state III to state IV).*** The decrease in $\bar{N}_1$ by ≈56% (see Fig. 4*A*) between pH 7.0 and 9.5 is responsible for the decrease in fluorescence intensity observed on the fluorometer. Because ε_1 remains constant and no additional species appear, a fraction of species 1 must enter a dark state during the alkaline transition (Fig. 5 *A* and *B*). Interestingly, not all molecules enter this dark state, because $\bar{N}_1$ reaches a limiting value at pH 9.5 ($\bar{N}_1 = 4.3$). Here, we observe the coexistence of two conformational states, one represented by ε_1 and the other represented by a dark state (Fig. 5*B*). We speculate that these two conformational states correspond to the two alkaline conformers known to exist for

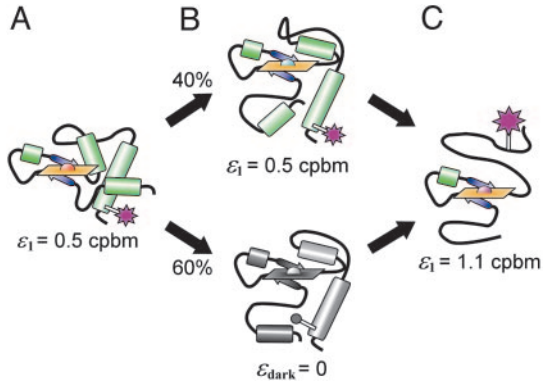

Fig. 5. Structural model for the pH-dependent conformations of TMR-cytochrome *c* resolved by PCH (see Fig. 4). (*A*) At pH 7.0, the fluorophore (magenta) has a brightness of $\varepsilon_1 = 0.5$ cpbm. (*B*) During the alkaline transition, 60% of species 1 enters a dark state and PCH resolves two discrete conformations. (*C*) As the protein unfolds, the fluorophore either brightens (*B Upper*) or leaves the dark state (*B Lower*) until ε_1 reaches a maximum of 1.1 cpbm.

yeast iso-1-cytochrome *c* (14), where either Lys-73 or Lys-79 is the sixth axial heme ligand (15). If this hypothesis is correct, PCH allows us to observe directly the transition into one of these two conformations through the decrease in $\bar{N}_1$. Studies on mutated cytochrome *c* could confirm these results by simplifying the conformational heterogeneity of the sample.

Unfolding cytochrome c (state IV to state V). The increase in intensity observed in fluorometer experiments between pH 9.5 and 10.8 is explained by increases in both $\bar{N}_1$ and ε_1 (Fig. 4). We would expect the fluorophore to become more exposed to solvent and also to move away from the heme group (a possible quencher) when molecules of TMR-cytochrome *c* unfold at highly alkaline pH (Fig. 5*C*). Both of these events should increase the brightness of the fluorophore to a value similar to TMR-cysteine. Although ε_1 never fully attains this brightness, it does increase by 110% from pH 9.5 to 10.8 (Fig. 4*C*). An increasing brightness indicates that PCH cannot resolve discrete values of ε for the folded and unfolded states. Two possible explanations exist for this result. Either the unfolding of cytochrome *c* proceeds through a number of intermediates (35) or the folded and unfolded states are in rapid equilibrium compared with the bin time of 20 μs. In either case, the brightness is a weighted average of these states. The dark state we attribute to one of the alkaline conformers is also expected to unfold under these conditions, thus reversing the previously described decrease in $\bar{N}_1$. Exactly this behavior is observed as $\bar{N}_1$ increases by 150% from pH 9.5 to 10.8 (Fig. 4*A*). Aggregation of TMR-cytochrome *c* begins to occur near pH 11 and precludes measurements at higher pH.

These experiments demonstrate the ability of PCH to measure the relative intensity contributions from $\bar{N}_i$ and ε_i, a distinct advantage over characterizing the fluorescence response by a single average intensity. Unlike the alkaline transition, where discrete states are resolved based on brightness, ε_1 gradually changes during the unfolding transition. PCH shows that either a continuum of unfolding intermediates exists for TMR-cytochrome *c* or the folded and unfolded states are in rapid equilibrium.

PCH Achieves Resolution Not Possible with Ensemble Fluorometry. As a final test of the resolving power of PCH, we measured PCH titration curves for two samples of TMR-cytochrome *c* with markedly different ensemble responses. The first sample was labeled with a 1:5 molar ratio of TMR/cytochrome *c* and gave a robust ensemble response of −40% for the alkaline transition (Fig. 6*A*). The second was labeled with a 2:1 molar ratio and gave a response of only −5% (Fig. 6*B*). As described above, we attribute this difference to the large background from doubly labeled species 2 present in the 2:1 labeled sample. The PCH titration curves for the relevant parameter ($\bar{N}_1$ for the alkaline transition) show a response of nearly the same magnitude in both samples (Fig. 6 *C* and *D*). For the 2:1 labeled sample, the response visualized by $\bar{N}_1$ improves an order of magnitude over the ensemble response (Fig. 6 *B* versus *D*). Thus, we demonstrate that PCH can dramatically improve the resolution of a fluorescence experiment by minimizing the effect of background interference, which allows examination of only the most relevant parameter(s).

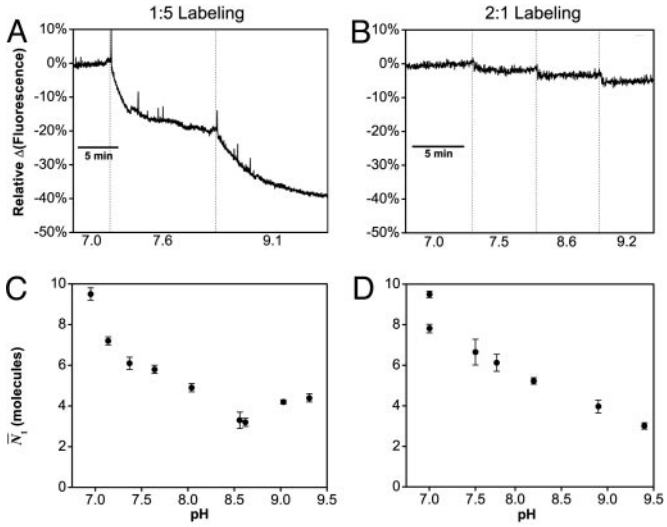

Fig. 6. The alkaline transition of TMR-cytochrome *c* as observed by ensemble fluorometry (*Upper*) and PCH (*Lower*). (*A* and *B*) Cytochrome *c* labeled at the optimal ratio of 1:5 shows a 40% decrease in fluorescence for the alkaline transition (*A*), whereas that labeled with a 2:1 ratio shows only a 5% decrease because of background from nonfunctional protein (*B*). (*C* and *D*) Regardless of the background, the $\bar{N}_1$ parameter from PCH shows a decrease of similar magnitude (−56% and −68%) for samples labeled at molar ratios 1:5 (*C*) and 2:1 (*D*).

We thank Brian Kobilka, Samuel Kim, Stephen J. Wrenn, and the Stanford University Mass Spectrometry staff for their help. T.D.P. is grateful for a Franklin Veatch Memorial Fellowship. M.P.B. is grateful for funding from the Medical Scientist Training Program (Stanford University School of Medicine). This work was supported by National Science Foundation Grant BES-0508531.

1. Vauquelin, G. & Van Liefde, I. (2005) *Fundam. Clin. Pharmacol.* **19,** 45–56.
2. Swaminath, G., Deupi, X., Lee, T. W., Zhu, W., Thian, F. S., Kobilka, T. S. & Kobilka, B. (2005) *J. Biol. Chem.* **280,** 22165–22171.
3. Zhuang, X. W., Kim, H., Pereira, M. J. B., Babcock, H. P., Walter, N. G. & Chu, S. (2002) *Science* **296,** 1473–1476.
4. Chen, Y., Müller, J. D., So, P. & Gratton, E. (1999) *Biophys. J.* **77,** 553–567.
5. Perroud, T. D., Huang, B., Wallace, M. I. & Zare, R. N. (2003) *ChemPhysChem* **4,** 1121–1123, and erratum (2003) **4,** 1280.
6. Huang, B., Perroud, T. D. & Zare, R. N. (2004) *ChemPhysChem* **5,** 1523–1531.
7. Perroud, T. D., Huang, B. & Zare, R. N. (2005) *ChemPhysChem* **6,** 905–912.
8. Lakowicz, J. R. (1983) *Principles in Fluorescence Spectroscopy* (Plenum, New York).
9. Magde, D., Elson, E. L. & Webb, W. W. (1974) *Biopolymers* **13,** 29–61.
10. Eigen, M. & Rigler, R. (1994) *Proc. Natl. Acad. Sci. USA* **91,** 5740–5747.
11. Chah, S., Kumar, C. V., Hammond, M. R. & Zare, R. N. (2004) *Anal. Chem.* **76,** 2112–2117.
12. Moore, G. R. & Pettigrew, G. W. (1990) *Cytochromes c: Evolutionary, Structural, and Physicochemical Aspects* (Springer, Berlin).
13. Theorell, H. & Åkesson, Å. (1941) *J. Am. Chem. Soc.* **63,** 1804–1820.
14. Hong, X. L. & Dixon, D. W. (1989) *FEBS Lett.* **246,** 105–108.
15. Ferrer, J. C., Guillemette, J. G., Bogumil, R., Inglis, S. C., Smith, M. & Mauk, A. G. (1993) *J. Am. Chem. Soc.* **115,** 7507–7508.
16. Silkstone, G. G., Cooper, C. E., Svistunenko, D. & Wilson, M. T. (2005) *J. Am. Chem. Soc.* **127,** 92–99.
17. Dickerson, R. E. & Timkovich, R. (1975) in *The Enzymes*, ed. Boyer, P. D. (Academic, New York), Vol. XI, pp. 397–547.
18. Döpner, S., Hildebrandt, P., Rosell, F. I. & Mauk, A. G. (1998) *J. Am. Chem. Soc.* **120,** 11246–11255.
19. Barker, P. D. & Mauk, A. G. (1992) *J. Am. Chem. Soc.* **114,** 3619–3624.
20. Rosell, F. I., Ferrer, J. C. & Mauk, A. G. (1998) *J. Am. Chem. Soc.* **120,** 11234–11245.
21. Louie, G. V., Hutcheon, W. L. & Brayer, G. D. (1988) *J. Mol. Biol.* **199,** 295–314.
22. Moench, S. J. & Satterlee, J. D. (1995) *J. Protein Chem.* **14,** 567–582.
23. Ravdin, P. & Axelrod, D. (1977) *Anal. Biochem.* **80,** 585–592.
24. Looze, Y., Polastro, E., Gielens, C. & Leonis, J. (1976) *Biochem. J.* **157,** 773–775.
25. Bryant, C., Strottmann, J. M. & Stellwagen, E. (1985) *Biochemistry* **24,** 3459–3464.
26. Moench, S. J. & Satterlee, J. D. (1989) *J. Biol. Chem.* **264,** 9923–9931.
27. Wilson, M. T. & Greenwood, C. (1996) in *Cytochrome c: A Multidisciplinary Approach*, eds. Scott, R. A. & Mauk, A. G. (University Science Books, Sausalito, CA), pp. 611–634.
28. Brewer, C. F. & Riehm, J. P. (1967) *Anal. Biochem.* **18,** 248–255.
29. Motonaga, K., Misaka, E., Nakajima, E., Ueda, S. & Nakanish, K. (1965) *J. Biochem.* **57,** 22–33.
30. Endo, S., Nagayama, K. & Wada, A. (1985) *J. Biomol. Struct. Dyn.* **3,** 409–421.
31. Müller, J. D., Chen, Y. & Gratton, E. (2000) *Biophys. J.* **78,** 474–486.
32. Ha, T. (2001) *Methods* **25,** 78–86.
33. Kapanidis, A. N. & Weiss, S. (2002) *J. Chem. Phys.* **117,** 10953–10964.
34. Jager, M., Michalet, X. & Weiss, S. (2005) *Protein Sci.* **14,** 2059–2068.
35. Bai, Y. W., Sosnick, T. R., Mayne, L. & Englander, S. W. (1995) *Science* **269,** 192–197.